Theor Chem Acc (2006) 115: 177–189
DOI 10.1007/s00214-005-0053-5

REGULAR ARTICLE

**María Luisa San-Román · Mauricio Carrillo-Tripp
Humberto Saint-Martin Jorge Hernández-Cobos
Iván Ortega-Blake**

A theoretical study of the hydration of Li^+ by Monte Carlo simulations with refined ab initio based model potentials

Received: 25 May 2005 / Accepted: 15 July 2005 / Published online: 19 January 2006

Abstract Four water models that have the same analytical potential but different degrees of freedom were used to examine the hydration of Li^+: (a) a polarizable and flexible molecule with constraints that account for the quantal nature of the vibration, (b) a polarizable and classically flexible molecule, (c) a polarizable and rigid molecule, and finally (d) a nonpolarizable and rigid molecule. The goal was to determine how individual molecular properties affect the correct description of the hydration of ions by comparing the structural and thermodynamic predictions for the aqueous solution as made by the different models, which ranged from a very refined one to a simple effective potential. The length of the Monte Carlo runs was large enough to ensure convergence and provide statistically meaningful results; the four models attained good agreement with the experimental data available for the hydration of Li^+, as well as with the results of the most refined simulations. A well-defined first hydration shell was found. It had four water molecules whose dipoles were not aligned to the electric field of the ion because of their hydrogen-bonding with water molecules in outer shells. In the case of the most refined water model, the results showed this pattern clearly. On the other hand, the rigid nonpolarizable version produced a slightly higher hydration number and an almost complete alignment of the dipoles to the ion's electric field. Moreover, a detailed analysis of a microscopic molecular model of hydration showed that the average intramolecular geometry of the water molecules in the first hydration shell was the same as the one for those in the bulk, whereas the electric field of the ion induced a dipole 0.2 D higher in the water molecules of the first hydration shell. The value of the bulk was recovered at the second shell, which explains the good performance of the simplest model. Thus, despite the differences found in the description of the first hydration shell between the polarizable and the nonpolarizable models, the major effect on the polarization of the water molecules resulted from the water-water interaction.

Keywords Lithium ion hydration · Polarizable force fields · Monte Carlo simulation

M.L. San-Román
Centro de Investigaciones Químicas,
Universidad Autónoma del Estado de Morelos,
Av. Universidad 1001, Col. Chamilpa,
Cuernavaca 62210, Morelos,
México

M. Carrillo-Tripp
Chemistry Department,
Wabash College, P.O.Box 352, IN,
Crawfordsville 47933,
USA

H. Saint-Martin · J. Hernández-Cobos · I. Ortega-Blake
Centro de Ciencias Físicas,
Universidad Nacional Autónoma de México,
Apartado Postal 48-3,
Cuernavaca 62251,
Morelos, México

I. Ortega-Blake (✉)
Departamento de Física Aplicada,
Centro de Investigación y Estudios Avanzados,
Unidad Mérida, Cordemex, Mérida 97310, Yucatán, México
E-mail: iortega@mda.cinvestav.mx

1 Introduction

Nowadays, numerical simulations are a powerful tool for the study of physicochemical systems at the molecular level, in particular those involving small molecules like the aqueous solutions of atomic ions. It is now clear that, with the use of refined potentials, simulations can yield results that are in good agreement with the reported experimental data. This gives confidence to observations that are not amenable to experimental determination, such as the molecular details of the hydration of single ions. Single hydration of atomic ions can be readily done in simulations, whereas experimental data are obtained from the solution of salts and then extrapolated to the hypothetical standard state of infinite dilution, where no ion-ion interactions take place [51].

The hydration of the lithium ion has received considerable attention given the many technological applications of Li^+ in batteries, alloys and lubricants, as well as its use in the treatment of psychiatric disorders and viral diseases – the applications of lithium have been recently reviewed by Birch [7] . On the other hand, the study of the lithium ion is also very attractive from the academic viewpoint; because of its size, it permits the use of a very refined quantum mechanical (QM) level to study its interaction with small molecules such as water [21,22,25] . This has led to multiple theoretical studies regarding the structural and energetic aspects of its hydration [16,17,45,48,63,71,81,82,84, 86]. Experimental studies of this phenomenon have also been undertaken, although there are discrepancies in the reported data. Specifically, the hydration number (i.e., the number of water molecules in the first hydration shell of the ion), has ranged from 3.3 to 6.5 depending on the concentration of LiCl in neutron scattering experiments [35,61], where the low values have been observed only at very large concentrations. Diffraction experiments [58,59,64,85] have reported a value of 4 similar to that of other lithium salts [11, 49], regardless of concentration. Raman spectroscopy further adds to disagreement by favoring the four molecule coordination.

Numerical simulations would be expected to help solve the problem, mainly in the low concentration limit. But simulations have also predicted values ranging from 4 to 6. There is a general trend indicating that pairwise simple potentials favour the larger limit [16,17,84,86], while more recent and refined methods such as Car-Parrinello molecular dynamics (CPMD) [48], QM/MM (molecular mechanical) molecular dynamics (MD) [45], and the quasi-chemical theory of liquids (QCTL) [71] favour a hydration of four, even for the infinite-dilution limit. Spångberg and Hermansson studied the hydration of Li^+ in a recent work [81,82], with potentials ranging from the pairwise expression to the inclusion of nonadditivity and polarizability. Their results show a clear trend from the upper to the lower reported hydration numbers in correlation with the successive complexity of the models. A value of four is found with the potentials that include nonadditive effects and polarizability, the importance of which has been shown in various studies of the ion-water interaction [1,2,6,9,27,28,41,42,53–55,60,65,66].

This work presents a Monte Carlo (MC) study of the Li^+ hydration at high dilution (one ion and 999 waters). It uses a very refined potential whose results are in good agreement with the experimental observations of water under various different thermodynamic conditions [33,74,76] as well as of aqueous solutions of ions [1,2,9,10]. Simulations are also presented using the same model, though intramolecular geometry and/or polarization were restricted to the average values produced by the model in simulations of liquid water [75]. The modelling of the Li^+–H_2O interaction is validated by comparison to the available experimental data in the gas-phase and in the aqueous solution. This is followed by a detailed analysis of the microscopic structure of the hydrated ion.

2 Methods

Numerical simulations were performed using the MC method. As in the previous study [9] of Na^+ and K^+, the MCDHO [74] analytical potential was used for the water–water interactions and the same type of model was employed for the water–cation interactions. This model represents the electron cloud of a molecule as a negative mobile charge density with radial exponential decay attached to a positively charged point core by a harmonic oscillator. The functional form has been presented elsewhere [9,75], and it allows the restriction of intramolecular flexibility and polarizability while simultaneously keeping the same set of parameters; thus, it is possible to separately study the effects that the inclusion of those degrees of freedom has on the results of the simulation [1,2,75]. To this end, MC simulations were performed with the four versions of MCDHO reported in Refs. [75] and [34], viz. $MCDHO_{ff}$, $MCDHO_{fc}$, $MCDHO_r$ and MCD.

2.1 The fitting procedure

The parameters for the Li^+–water interaction were fitted to reproduce the experimental polarizability of the ion [51], $\alpha = 0.0317$ Å^3, the potential energy surface (PES) built with ab initio calculations of the pair interactions, and the three- and four-body nonadditive contributions to the interaction energy, computed with ab initio calculations of trimers and tetramers.

The calculations of the pair-interaction were performed at the MP2(CP)/6-311++G($3df$, $3p$) level of the theory; that is, the second order many-body perturbation theory with counterpoise correction [8]. This was also chosen previously [9] because it yields the right polarizability and dipole moment of H_2O; it also yields the right polarizability of Li^+. All quantum calculations in this work were done with the GAUSSIAN98 [24] program.

The Li^+–H_2O interaction has been studied extensively by Feller et al. [21,22] and Glendening and Feller [25] who estimated the complete-basis-set limit (CBS) at the fourth-order many-body perturbation theory (MP4) level of the interaction energy to be $\Delta E = -35.0\,\mathrm{kcal\,mol^{-1}}$. The calculations of Spångberg and Hermansson [81], on the other hand, yield $\Delta E = -33.5\,\mathrm{kcal\,mol^{-1}}$ at the MP2(CP)/TZV++($3df$, $3p$) level. The calculations performed here resulted in $\Delta E = -33.0\,\mathrm{kcal\,mol^{-1}}$.

The final values of the parameters are presented in Table 1, using the notation of Ref. [9]; only nonzero values are shown. It should be stressed that this set of parameters is not unique; other values could produce a similar adjustment to the ab initio data, and more parameters could also be used. The additional criteria for the selection of the values in this work were the following: (1) to use integers for the core and the mobile charges of Li^+; once q was chosen, the spring constant was determined from the polarizability as $k = q^2/\alpha$; (2) to keep the 12-6 exponents in the Lennard–Jones terms between the mobile charge of the ion and that

of the water molecule, and (3) to use the minimum possible number of parameters to reproduce the ab initio computed energies. There are thus four independent free parameters: the mobile charge of the ion, q, the decay length λ', and the Lennard–Jones coefficients α_{Li-O} and β_{Li-O}. The parameters q and λ' were initially chosen to yield the best possible reproduction of the interaction energy and the Li^+–O distance of the optimal dimer, and α_{Li-O} and β_{Li-O} were used to improve the agreement with the ab initio values. This set of parameters was used to generate $Li^+(H_2O)_n$ clusters, with $n = 1, 2, \ldots, 6$, from which the three- and four-body nonadditive contributions were calculated at the HF(CP)/6-311++G($3df, 3pd$) level of the theory. The correlation energy was neglected in these calculations because it is mostly additive [9,46]. The parameters were then readjusted to a total of 746 points in the pair interaction PES, and 146 three-body and 246 four-body nonadditive contributions to the energy. These points included a sample along the line of optimal Li^+–H_2O orientation, and configurations with deformed water molecules; thus the intramolecular energy was considered in the many-body expansion of the interaction energy [9,68].

The plot in Fig. 1a shows the behavior of the model along the line of optimal Li^+–H_2O orientation, compared to the ab initio values; the geometry of the water molecule was fully optimized for each Li^+–O distance. As previously reported [9], after 5 Å the interaction is purely electrostatic. For distances shorter than 1.6 Å, the model exaggerates the repulsion due to the short-range Lennard–Jones term. However, at that distance the ab initio energy is already 10 kcal mol^{-1} above the minimum and the slope of the curve is large enough as to assume that this region will not be importantly sampled in a simulation of the aqueous solution under ambient conditions. On the other hand, the comparison to the 746 points in the ab initio pair interaction PES, at distances longer than 1.7 Å, is shown in Fig. 1b. The slope of the linear regression, $m = 0.994$, and the mean-square-error attained, $e_{\rm rms} = 0.4$ kcal mol^{-1}, were deemed satisfactory. Further attempts to add Lennard–Jones terms to the Li^+–H interaction did not result in any significant improvement, nor did the use of exponents other than 12-6, nor the use of a Buckingham short-range term.

In regard to the three- and four-body nonadditive contributions, the agreement of the model with the ab initio calculations was less satisfactory: the model overestimated the three- and the four-body nonadditivities by 20% and 55% respectively. The four-body contributions are small (∼0.5 kcalmol^{-1}) and the three-body are reasonably well reproduced. Because Li^+ is practically nonpolarizable, it has been shown that the nonadditive contributions to the interaction stem mainly from the polarizability of the water molecule [43]; hence a better agreement could not only be obtained by modifying the water model. The comparison of the model's nonadditive contributions to the ab initio values is shown in Fig. 2a, b. The slope of the linear regression in Fig. 2a is $m = 1.1917$ with a standard error of $e_{rms} = 0.6$ kcal mol^{-1}, whereas the corresponding values in Fig. 2b are $m = 1.545$ and $e_{rms} = 0.14$ kcal mol^{-1}. Though exaggerated, the three- and four-body nonadditive contributions to the energy produced by the model are in agreement with the ab initio

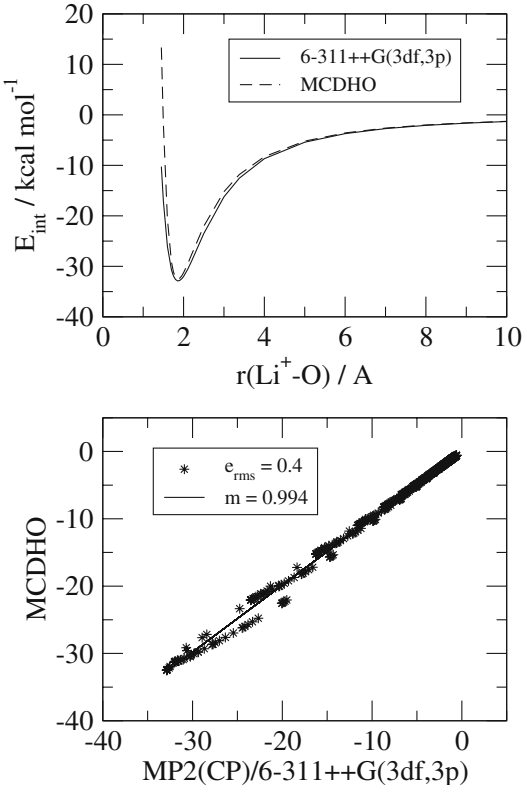

Fig. 1 Comparison of the model to the ab initio pair interaction energies. *Top*: Along the line of optimal $Li^+ - H_2O$ approach. *Bottom*: To the 746 points in the PES

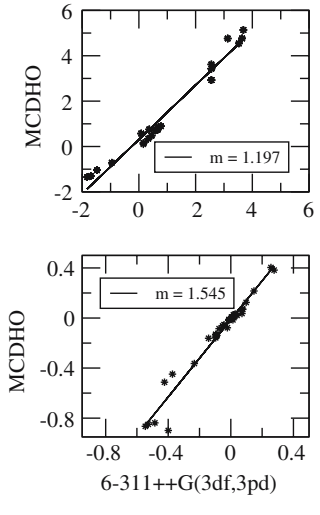

Fig. 2 Comparison of the model to the ab initio non-additive contributions to the interaction energy. *Top*: Three-body contributions. *Bottom*: Four-body contributions. All energy in kcal mol^{-1}

Table 1 Parameters for the Li^+–H_2O interaction in a.u. Only nonzero parameters are presented

Z	3.0
q	−2.0
k	18.691316
λ'	0.773426
$\alpha_{Li–O}$	14000.0
$\beta_{Li–O}$	−13.0

The definition of each parameter corresponds to the analytical potential of Refs. [9] and [75]

data within the limits of thermal fluctuations at $T = 298$ K. Thus, it was decided to use the model with the parameters of Table 1.

3 Results

3.1 Small clusters

To test the reliability of the models and their parametrization, their predictions of the interaction energy for various different $Li^+(H_2O)_n$ clusters ($n = 1, 2, \ldots, 6$) were compared to ab initio calculations [21,22,25] and gas-phase experimental data [18,72]. In the case of the dimer ($n = 1$), the geometrical parameters were also compared along with the water dipole moment (Table 2). It is worth mentioning that there is no unique way of assigning electrical properties to individual molecules from ab initio calculations of clusters. However, the quantum theory of atoms in molecules [3], based on the analysis of the topological properties of the electron density, provides a reasonable framework to assign charges to different sites. This method was used in this case to estimate the water dipole moment from the MP2(CP)/6-311++G($3df, 3p$) calculation, as was the case in previous studies [74].

Table 2 presents a comparison between the predictions for the Li^+–H_2O dimer at the best ab initio level [21], the one computed in this work at the MP2(CP)/6-311++G($3df, 3p$) level, and those predicted by the classical models used in this work.

Of course, the ab initio interaction and the Li^+–O distance computed in this work were well reproduced by the MCDHO model since they were used in the fitting procedure. But the intramolecular geometry of the water molecule in the dimer and its dipole moment were not fitted. The flexible model for water produced a longer r(O–H) bond than the ab initio calculation and a somewhat larger dipole. The rigid polarizable $MCDHO_r$ model reproduced the energy and the separation quite well, with an even larger dipole for water. The nonpolarizable MCD model yielded a slightly longer separation and underestimated the interaction energy by 6%. Because the parameters of the MCDHO models were not readjusted in this work, the longer bonds and narrower bond angle produced by them can be ascribed to some extent to the parametrization with a different water monomer deformation PES [74]. This different geometry, in turn, affects the dipole moment. Even if the differences found with the $MCDHO_{fc}$ model amounted to only 2% in the bond length and less than 1% in the bond angle, the difference in the dipole moment amounted to 15%.

The interaction energies of larger clusters are shown in Table 3, where the geometries are represented in terms of the number of water molecules in the first and second hydration shells, n_1 and n_2, respectively, and they correspond to Fig. 1 of Ref. [25]. The ab initio results presented in this work and those of the classical models were compared to the best ab initio values [25]. The configurations were optimized with each version of the MCDHO model in all cases, whereas it was only possible to make full ab initio optimizations for clusters with up to $n = 4$ water molecules. For the larger clusters single-point ab initio calculations were performed with the configurations optimized with $MCDHO_{fc}$, and the CP correction was applied to obtain the interaction energies. As it should be expected from the comparison with the dimer, all MP2(CP)/6-311++G($3df, 3p$) interactions turned out smaller than the best ab initio value [25]: for $n = 1, 2$ the difference is roughly 1.5 kcal mol^{-1}, and it increases up to 4 kcal mol^{-1} for $n = 3, 4$. The larger discrepancies for $n = 5, 6$ stem from using the optimal geometries produced by $MCDHO_{fc}$, which do not correspond to the optimal ab initio geometries.

In regard to the performance of the model, the four versions were able to produce the right configurations as stable local minima in their respective energy surfaces, albeit with somewhat different geometric parameters (distances and angles). Generally speaking, there was a fairly good agreement with the ab initio values obtained in this study, again smaller than the best calculations. However, as the number of water molecules increases, the water–water hydrogen-bonding becomes more important, in the absence of direct interaction with the ion. This is reflected in a smaller difference relative to the best calculations in the interaction energy for the six-water cluster than would be expected from the Li^+–H_2O pair. Even the nonpolarizable MCD model kept some of this nonadditivity, as explained in Ref. [75].

A further validation of the models can be made by comparing their predictions of the enthalpies of succesively larger clusters at $T = 298$ K, ΔH^{298}_{hyd}, to the theoretical and experimental data reported in the literature. This was done by performing MC simulations of the clusters, and using the ideal-gas formula [1,15,81]

$$\Delta H = \Delta U + p\Delta V = \Delta U - nRT, \tag{1}$$

where $p = 1$ atm is the pressure, n is the number of water molecules in the cluster, R is the gas constant, and $T = 298$ K the temperature. The results are presented in Table 4, showing

Table 2 Comparison to ab initio data of the interaction energy and the geometrical parameters of the optimal Li^+–H_2O dimer produced by the models

	Est. CBS[a]	This work[b]	$MCDHO^c_{fc}$	$MCDHO_r$	MCD
E_{int}	−35.2	−33.0	−33.3	−33.2	−31.0
r(Li^+–O)	1.847	1.8593	1.8525	1.8523	1.8931
r(O–H)	0.962	0.9631	0.9832	0.9840	0.9840
∠HOH	105.0	105.5	104.9	102.7	102.7
μ_{H_2O}		3.11[d]	3.60	3.65	2.96

The energy is in kcal mol^{-1}, the distances are in Å, the angle in degrees and the dipole moment in Debye
[a]Estimated complete basis set limit MP2 from Refs. [21,22]
[b]Optimized with MP2(CP)/6-311++G($3df$, $3p$)
[c]The optimal dimer is the same for $MCDHO_{ff}$
[d]Computed from the charges obtained with the atoms-in-molecules method [3]

Table 3 Comparison to ab initio data of the interaction energy of the optimal Li^+–$(H_2O)_n$ clusters produced by the models ($n = 1, \ldots, 6$)

n	Geometry	Ref. [25][a]	This work[b]	$MCDHO^c_{fc}$	$MCDHO_r$	MCD
1	1+0 (C_{2v})	−34.5	−33.0	−33.3	−33.2	−31.0
2	1+1 (C_s)	−51.5	−49.8	−52.6	−51.7	−46.4
	2+0 (D_{2d})	−64.4	−63.1	−61.0	−60.7	−58.4
3	2+1 (C_s)		−76.8	−78.0	−77.2	−72.6
	2+1 (C_2)	−80.2		−76.9	−76.3	−74.0
	3+0 (D_3)	−87.5	−84.0	−81.0	−80.6	−79.8
4	3+1 (C_2)	−103.1	−97.8	−97.7	−97.0	−92.4
	4+0 (S_4)	−104.1	−100.4	−96.4	−95.6	−94.8
5	4+1 (C_2)	−118.5	−111.4[d]	−112.3	−111.5	−109.4
6	4+2 (C_s)	−130.9	−120.7[d]	−127.1	−126.0	−121.5

The geometries are represented as $n_1 + n_2$, where n_1 is the number of molecules in the first hydration shell and n_2 the number of molecules in the second hydration shell. The energies are in kcal mol^{-1}, and the geometries are those of Ref. [25]
[a]Counterpoise corrected values MP2(CP)/6-31+G*//RHF/6-31+G*
[b]Computed with MP2(CP)/6-311++G($3df$, $3p$) on configurations optimized with the same level of the theory for $n = 1, 2, 3, 4$, and on the configurations optimized with $MCDHO_{fc}$ for $n = 5, 6$
[c]The optimal clusters are the same for $MCDHO_{ff}$
[d]Geometries optimized with the $MCDHO_{fc}$ model

Table 4 Comparison to experimental data (second and third columns) and theoretical ab initio estimates (fourth column) of the cumulative enthalpy of the Li^+–$(H_2O)_n$ clusters produced by the models in gas-phase simulations at T = 298.15 K ($n = 1, \ldots, 6$)

n	HPMS[a]	CID[b]	Ab initio[c]	$MCDHO_{fc}$	$MCDHO^d_{ff}$	$MCDHO_r$	MCD
1	−34.0	−32.7	−34.2	−33.1	−32.9	−33.0	−30.6
2	−59.8	−60.0	−61.7	−60.2	−60.0	−60.0	−56.9
3	−80.8	−82.5	−83.4	−79.4	−79.5	−79.0	−77.7
4	−96.9	−99.4	−98.6	−93.0	−92.8	−93.1	−91.7
5	−110.8	−113.8	−111.7	−104.2	−104.5	−104.2	−102.0
6	−122.9	−128.8	−122.4	−116.1	−115.0	−114.5	−110.1

The enthalpies were estimated with the ideal gas formula [15,1,81] $\Delta H = \Delta U + p\Delta V = \Delta U - nRT$, where n is the number of water molecules in the cluster. The values are in kcal mol^{-1}
[a]High-pressure mass spectrometric measurements [18]
[b]Collision-induced dissociation data [72]
[c]Ab initio calculations with large correlation-corrected basis sets [21]
[d]An energy of $(3/2)RT$ per molecule was added to correct for the classical sampling of the intramolecular degrees of freedom

the same behavior as in Table 3. For a more refined analysis, the enthalpies of the detachment reactions

$$Li^+(H_2O)_n \rightarrow Li^+(H_2O)_{n-1} + H_2O \quad (2)$$

are plotted in Fig. 3. Though the models' values were systematically lower than the experimental data, the qualitative behavior of $MCDHO_{fc}$ was the same as that of the collision-induced dissociation data (CID) since the enthalpy change from $n = 6$ to $n = 5$ is higher than from $n = 5$ to $n = 4$. A general feature found with the four models was that, in agreement with the ab initio data, they favoured a four-membered first hydration shell, given that the optimal configurations of larger clusters all have $n_1 = 4$ (Table 3).

The previous comparison led to the conclusion that the model was suitable for numerical simulations of the aqueous solution under ambient conditions.

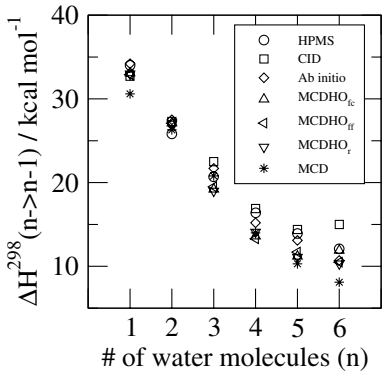

Fig. 3 Enthalpies of the detachment reactions $Li^+(H_2O)_n \rightarrow Li^+(H_2O)_{n-1}+H_2O, n = 1, 2, \ldots, 6$, in kcal mol^{-1}. *HPMS*: High-pressure mass spectroscopy [18]; *CID*: Collision-induced dissociation [72]; ab initio data from Ref. [25]

3.2 Aqueous solution

Following the procedure described in Ref. [9], MC simulations with the Metropolis algorithm [29,57] were performed on the NVT ensemble at $T = 298.15$ K, for a system of 999 water molecules and one Li^+ ion in a cubic cell of V = 29915 Å^3, thus a density of ρ =0.999 g cm^{-3}. A simulation of the same system was performed with each of the four versions of the MCDHO model. In all cases the lithium ion was considered polarizable, although its polarizability is very low. To explore a larger region of the configurations' space, each of the four simulations was distributed in five CPU's, as described in Ref. [75]. A spherical cutoff radius of $R_c = 10.85$ Å was used for the intermolecular interactions, as well as periodic boundary conditions with Ewald sums [20] to account for long-range electrostatics. The adiabatic nuclear and electronic sampling (ANES) [12,52] scheme was used to treat the polarizability of MCDHO$_{ff}$ and of MCDHO$_r$, as well as the polarizability and flexibility of MCDHO$_{fc}$ (using T_{qm}=0.05 K and a sampling ratio quantum:classical of 10:1). The blocking method of Flyvbjerg and Petersen [23] was used to make sure convergence was attained and statistical sampling was significant. The hydration enthalpy $\Delta H_{\rm hyd}$ was computed as the difference between the average of the total interaction energy of the system, $< E_{\rm S} >$, and n times the average energy of a single water molecule, $< E_{\rm H_2O} >$, i. e.,

$$\Delta H_{\rm hyd} =< E_{\rm S} > -n < E_{\rm H_2O} >, \qquad (3)$$

where $n = 999$ is the number of water molecules in the system. This is a small difference between two large values, $\Delta H_{\rm hyd}$ being only a hundredth of the total energy of the system, and therefore very sensitive to the choice of $< E_{\rm H_2O} >$. To ensure that the reference value had exactly the same conditions as the aqueous solution, it was chosen as the average energy of the water molecules located at distances longer than 7 Å within the same simulation of the ion, instead of the average obtained from previous simulations of pure water [75]. This procedure has been applied successfully in previous studies of various different solutes [31,32,77]. Besides, the discrepancy turned out to be less than 0.1 kcal mol^{-1} per molecule for the four models.

The graph at the top of Fig. 4 shows the cumulative average of the predicted hydration enthalpy as a function of the number of MC cycles (1 $N_{\rm cycle} = 10^3$ configurations), after an equilibration period of 2.5×10^5 $N_{\rm cycles}$. The bottom graph of Fig.4 shows that a plateau was reached for the standard deviation of each model, making the sample statistically meaningful.

The energetic and structural parameters of the Li^+ hydration obtained from the simulations in this work are compared to experimental data in Table 5, and to the results of other simulations and theoretical calculations in Table 6. As discussed by Grossfield [26], the experimental estimates of the hydration enthalpy vary as much as 20 kcal mol^{-1} from one another, because they depend on the partition scheme used to distribute the hydration enthalpy of the salt among the resulting solvated ions. Yet, the values obtained from the simulations in this study lie within the extremes and can thus be considered in as good agreement with the experimental data as the most refined theoretical results [45,48,71,81,82].

Another issue of discussion regards the hydration number [86]. As previously mentioned, the estimates made from experimental data range from 3.3 to 6.5 and seem to depend strongly on the salt concentration [35,61], though X-ray diffraction [59,85] and Raman spectroscopy [38,73] yield a hydration number of four. This is also the case of the most recent and refined numerical simulations and theoretical

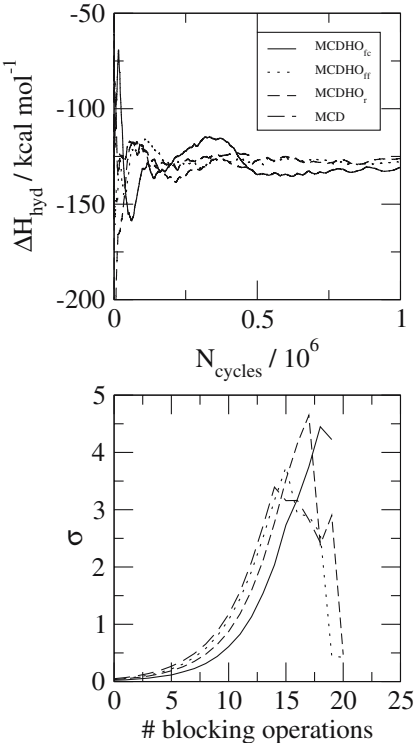

Fig. 4 *Top*: Cumulative solvation energy versus number of Monte Carlo cycles. *Bottom*: The corresponding standard deviations versus the blocking operations

Table 5 Li^+ hydration energetic and structural properties obtained from the simulations in this work, compared to the experimental data reported in the literature

	n_{H_2O}/n_{Li}	$-\Delta H_{hyd}$	$< n >$	r_{MO}	r_{MH}	ϕ
CISD[a]		134				
NDIS[b]	5.6		3.3(5)	1.95(2)	2.50(2)	52(5)
NDIS[b]	15.6		5.5(5)	1.95(2)	2.55(2)	40(5)
MTDH[c]		127	5.2			
CISD[d]		138				
NDIS[e]	4.0		3.2(2)	1.96(2)	2.52(2)	
NDIS[e]	15.4		6.0(4)	1.95(2)	2.52(2)	
NDIS[e]	55.6		6.5(2)	1.96(2)	2.52(2)	
CISD[f]		138				
MTDH[g]		121		1.94–2.28		
FEIS[h]			5.1			
$MCDHO_{fc}$	999	129	4.0	1.97	2.54	40
$MCDHO_{ff}$	999	128	4.0	1.97	2.56	0
$MCDHO_{rc}$	999	127	4.0	1.97	2.54	0
MCD	999	125	4.3	1.99	2.65	0

The hydration enthalpy ΔH_{hyd} is in kcal mol^{-1}, and the distances in Å; r_{MO} is the location of the first peak of the radial distribution function $g_{Li-O}(r)$. The first maximum of $g_{Li-H}(r)$ is located at r_{MH}. ϕ is the angle (in degrees) between the dipole of the water molecule and the Li–O axis. The numbers in parentheses indicate the uncertainty in the last reported digit

[a] *CISD* Cluster ion solvation data, Ref. [40]

[b] *NDIS* Neutron diffraction and isotopic substitution, Ref. [61]

[c] *MTDH* Model for the thermodynamics of hydration, Refs. [50,51]

[d] *CISD* Cluster ion solvation data, Ref. [13]

[e] *NDIS* Neutron diffraction and isotopic substitution, Ref. [35]

[f] *CISD* Cluster ion solvation data, Ref. [83]

[g] *MTDH* Model for the thermodynamics of hydration, Ref. [78]

[h] *FEIS* Field evaporation of ions from solutions, Ref. [39]

Table 6 Li^+ hydration energetic and structural properties obtained from the simulations in this work, compared to the theoretical data reported in the literature

	n_{H_2O}/n_{Li}	$-\Delta H_{hyd}$	$< n >$	r_{MO}	$g_{Li-O}(r_M)$	r_m	r_{MH}	ϕ
MD-TIP4P[a]	150	125	5.9(3)	2.09(2)			2.57(2)	
MC-TIP4P[b]	124		5.8(4)	2.20	9.5	3.11	2.78	26
QCTL[c]		128	4.0	2.00				
CPMD[d]	32		4.0	1.96	8.5		2.58	40–50
MD-IMC[e]	256	100	4.0	1.96	7.0			
MD-SPC/E[f]	255		4.4	1.97	13.8	2.56		0
QM/MM-HF[g]	499		4.2	1.95	9.9	2.97		30
QM/MM-DFT[g]	499		4.1	1.93	9.9	2.71		40
MD-RWK2[h]	230	116	4.6	1.93	9.5			10–15
MD-3BP-SPC/E[i]	512	120	4.0	1.96	8.8	2.66	2.62	0
QCSM[j]	89		4.0	2.05		2.78	2.71	
$MCDHO_{fc}$	999	129	4.0	1.97	9.9	2.61	2.54	40
$MCDHO_{ff}$	999	128	4.0	1.97	9.7	2.64	2.56	0
$MCDHO_{rc}$	999	127	4.0	1.97	9.7	2.66	2.54	0
MCD	999	125	4.3	1.99	9.2	2.85	2.65	0

The hydration enthalpy ΔH_{hyd} is in kcal mol^{-1}, and the distances in Å; r_{MO} is the location of the first peak of the radial distribution function $g_{Li-O}(r)$, and r_m the following minimum. The first maximum of $g_{Li-H}(r)$ is located at r_{MH}. ϕ is the angle (in degrees) between the plane of the water molecule and the Li–O axis. The numbers in parentheses indicate the uncertainty in the last reported digit

[a] Molecular dynamics (MD) with the TIP4P model of water [37], Ref. [84]

[b] Monte Carlo (MC) simulation with the TIP4P model of water [37], Ref. [16]

[c] Quasi-chemical theory of liquids, Ref. [71]. The free energy $\Delta_{hyd}G$ is shown, instead of the enthalpy

[d] Car-Parrinello molecular dynamics simulation CPMD, Ref. [48]

[e] Molecular dynamics with the SPC model of water [5] and an effective potential for the Li^+–H_2O interaction, obtained with the inverse MC (IMC) method [47], Ref. [48]. The free energy $\Delta_{hyd}G$ is shown, instead of the enthalpy

[f] Molecular dynamics with the SPC/E model of water [4] and a Li^+–H_2O model of Pettitt and Rossky [69], Ref. [86]

[g] Quantum-mechanical molecular-mechanical (QM/MM) MD simulations, Ref. [45]

[h] Molecular dynamics with the RWK2 model of water [70], Ref. [17]

[i] Molecular dynamics with an effective three-body potential (3BP) based on the SPC/E model for water [4], Refs. [81,82]

[j] Combined quantum-chemical statistical-mechanical simulation, Ref. [63]

methods [45,48,71,81,82]. As shown below, the results of this work are in agreement with a hydration number of four.

The Li^+–O radial distribution functions (rdf's) are shown in the top graph of Fig. 5. The four models employed produced very similar results, with the small differences shown in the bottom graph. MCD produced the largest departure from MCDHO$_{fc}$. This was mainly due to the occurrence of its first maximum of $g_{\mathrm{Li–O}}(r)$ at a longer distance than those of the other models, which is consistent with the larger Li^+–OH_2 separation found previously for the pair (Table 2). In contrast to other singly-charged cations [9], a depletion zone similar to that produced by doubly-charged cations [6] was found. This was due to lithium's shorter hydration radius. The Li^+–H rdf also showed a first peak (Fig.6), suggesting a well defined first hydration shell, but without the depletion zone that is produced for instance by Mg^{2+} [6]. In this regard, Li^+ proved similar to Ca^{2+} [6], a result that is consistent with the mean lifetime of a water molecule in the first hydration shell of each of the three cations (see e.g. Fig. 1 of Ref. [30]) and with the fact that the classical "solventberg" model is adequate to describe the mobility of the Li^+ ion in water [43]. After the first hydration shell, a second one could be appreciated in both rdf's. There was even a third one gauging from the third peak of $g_{\mathrm{Li–H}}(r)$.

An estimate of the hydration number can be made from integrating $g_{\mathrm{Li–O}}(r)$ up to the first minimum. The result of this procedure is presented in Fig. 7a, where it can be seen that the three polarizable models yielded the same value of four, while MCD produced a somewhat higher prediction, 4.3. This discrepancy can be explained with the histogram in Fig. 7b: the three polarizable models kept four molecules in the first hydration shell for more than 90% of the simulation, with small departures to three and to five. Alternatively, in the case of the simulation with MCD a, first hydration shell of four amounted to less than 50% and hydration numbers of three, five or six also occurred. The results of the polarizable models were in good agreement with results from QM-MM-MD [45], with the QCTL [71] and with earlier predictions derived from ab initio calculations [21].

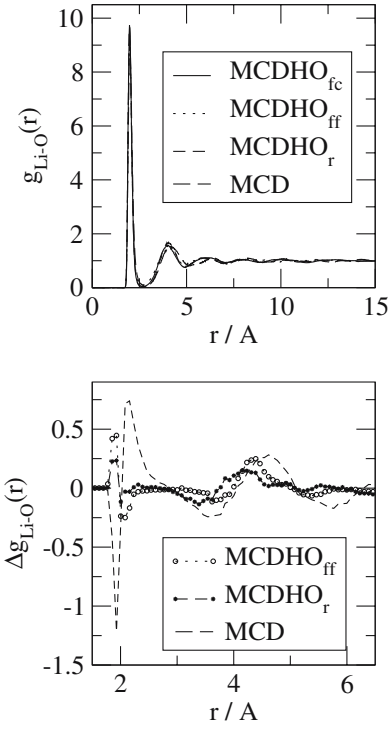

Fig. 5 *Top*: Radial distribution functions $g_{\mathrm{Li–O}}(r)$ produced by the four models. *Bottom*: difference relative to the results obtained with MCDHO$_{fc}$

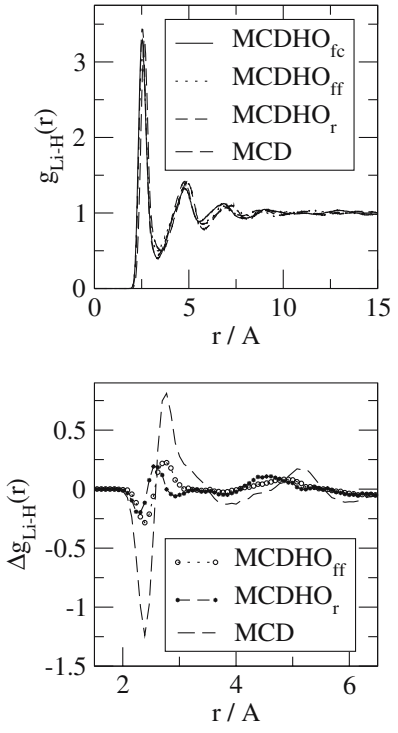

Fig. 6 *Top*: Radial distribution functions $g_{\mathrm{Li–H}}(r)$ produced by the four models. *Bottom*: Difference relative to the results obtained with MCDHO$_{fc}$

It is worth pointing out that even the simple MCD model yielded reasonably good energetic and structural results. Previously such performance had only been recorded by the effective pairwise potential of Zhou et al. [86], and by SPC/E [4] combined with the nonadditive ion–water potentials of Dang [15].

The distribution of the angle ∠O–Li–O for water molecules in the first hydration shell is shown in Fig. 8. In agreement with CPMD [48] and QM-MM-MD [45], the three polarizable models produced a maximum at 109.4°, evidence of a rather stable tetrahedral arrangement, with a tail toward wider angles, indicating the disruption of the structure by exchange reactions that altered the hydration number temporarily. On the other hand, the MCD model yielded a wider distribution with a maximum at 100.0° and a significant population around 180°, indicating the presence of planar arrangements. This last result is similar to the one obtained

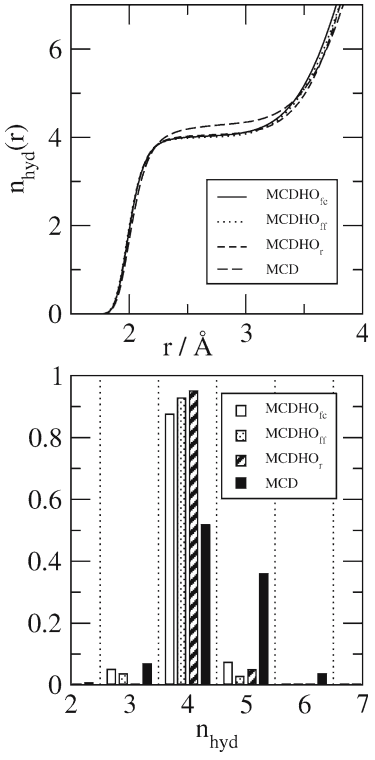

Fig. 7 *Top*: Cumulative number of water molecules $n_{\mathrm{hyd}}(r)$ obtained from integrating $g_{\mathrm{Li-O}}(r)$. *Bottom*: Histogram of the number of water molecules in the first hydration shell

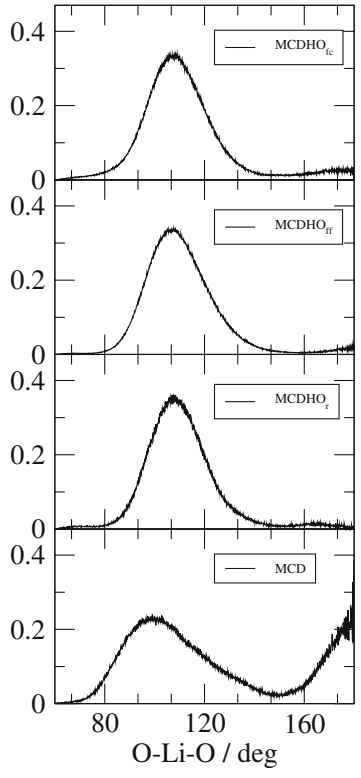

Fig. 8 Distribution of the angle O–Li–O among water molecules in the first hydration shell

by Duan and Zhang [17] with the flexible RWK2 model for water [70].

In order to determine the orientation induced on the water molecules by the ion's electric field, the angle ϕ between the position vector of the water's oxygen relative to the Li^+ ion, $\mathbf{r}_{\mathrm{Li-O}}$, and the dipole moment of the water molecule, $\boldsymbol{\mu}_{\mathrm{H_2O}}$, was computed. In the case of MCD this corresponds to the usually quoted tilt angle [48,61] between the $\mathbf{r}_{\mathrm{Li-O}}$ vector and the bisector of the $\angle$H–O–H angle (some authors use the supplementary angle [15,17,45,86]). The distributions of ϕ for each of the four studied models and each of the four regions (three hydration shells and the bulk) are shown in Fig. 9. MCDHO$_{fc}$ yields a maximum at $\phi \approx 40°$, in good agreement with neutron diffraction data [61] and simulations with QM force-fields [45,48]. MCDHO$_r$ had a local maximum at the same value of ϕ, whereas MCDHO$_{ff}$ only had a noticeable shoulder, a feature shared with less intensity by MCD. The behavior of the latter, nonpolarizable model resembled that of effective pair potentials, as in the case of Zhou et al. [86] –even if combined with nonadditive ion–water potentials [15].

Among the first attempts to explain the deviation from the alignment to the electric field, a specific interaction of Li^+ with a "lone-pair" of the water molecule was proposed [61]. The pair interaction obtained from ab initio calculations [21] has proved that interpretation to be wrong, as the optimal configuration corresponds to $\phi = 0$. Instead, the deviation can be ascribed to enhanced hydrogen-bonding between water molecules in the first and second hydration shells [9].

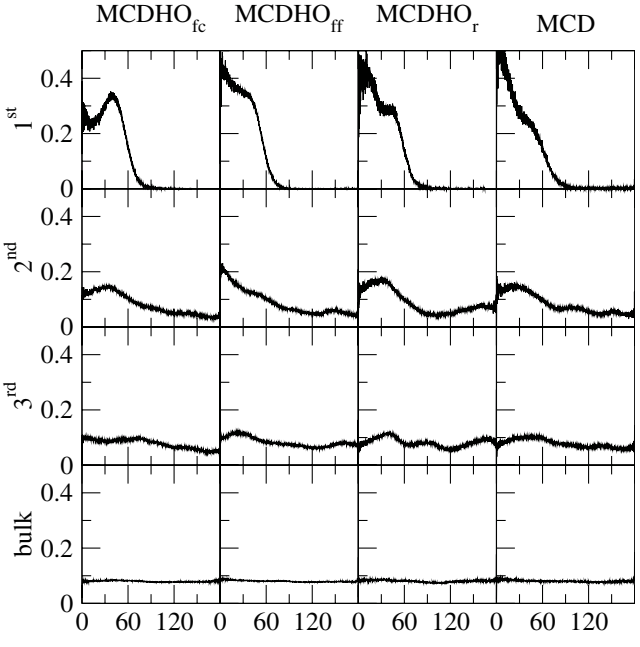

Fig. 9 Distribution of the angle between the electric field of the ion and the dipole moment of each water molecule in the first, second and third hydration shells, and the bulk, from *top* to *bottom*.

It is worth mentioning that in a recent interpretation of neutron diffraction data on aqueous solutions of hydroxides, at solute concentrations ranging from 1 solute per 12 water molecules to 1 solute per 3 water molecules, by means of Soper's empirical potential structure refinement (EPSR) technique [79,80], Imberti et al. [36] concluded that there was a rather strong alignment induced on the dipole moments of first-shell water molecules by the cation's electric field. While this happened with Li^+ and Na^+, in the case of K^+ they found the aforementioned 45° deviation. Moreover, they claim that their results on this alignment are in agreement with the CPMD simulations of Lyubartsev et al. [48], in spite of the latter authors' mention of a 40–50° deviation. Another discrepancy between Imberti's results and those from refined simulations, including those presented here, lies in the predicted structure of the first hydration shell: the first minimum of their Li^+–O rdf does not reach a value low enough to correspond to a depletion layer. This is in disagreement with previous experimental results on the residence time of a water molecule in the first hydration shell [30]. Though Imberti et al. [36] did not report the hydration number of any of the cations they studied, it is likely to be larger than four in the case of Li^+, gauging from their rdf's.

The EPSR technique involves refining a starting interatomic potential energy function in a way that produces the best possible agreement between the simulated and measured site-site partial structure factors [80]. But in order for EPSR to be successful the rdf's must uniquely determine the higher order correlation functions. This, in turn, can only occur in a pairwise additive system [19,80]. Thus, a possible explanation of the discrepancies mentioned above is the use of a rigid nonpolarizable model in the MC simulations of Imberti et al. [36]. As was previously mentioned, this study found that the MCD model does predict the alignment of the dipoles of first-shell water molecules to the ion's electric field.

Figure 9 shows that the water molecules in the second shell are still affected by the electric field of the ion, though to a much less extent. The orientation in the third shell is almost random, showing the effect to be short-ranged. Thus a completely random orientation was reached after 7 Å from the ion.

To analyze the effect of the ion's electric field on the individual water molecules, the per-molecule dipole moment was computed at each region. The corresponding distributions are presented in Fig. 10. It is clear that the induced dipole is 0.2–0.26 D higher for waters in the first hydration shell, as compared to the bulk, but the bulk value is recovered from the second shell onward. The effect of the ion's field on the intramolecular geometry is even lower. The graphs in Fig. 11 show that the r(O–H) bond-length and the $\widehat{\mathrm{HOH}}$ angle of the waters in the first hydration shell are only slightly different from those of bulk waters. Even the asymmetry between the two bonds shown in the rightmost graphs of Fig. 11 is identical in the first hydration shell to that in the bulk. This mild and short-ranged effect on the geometric properties of the water molecules explains the good performance of the rigid MCDHO$_r$ model.

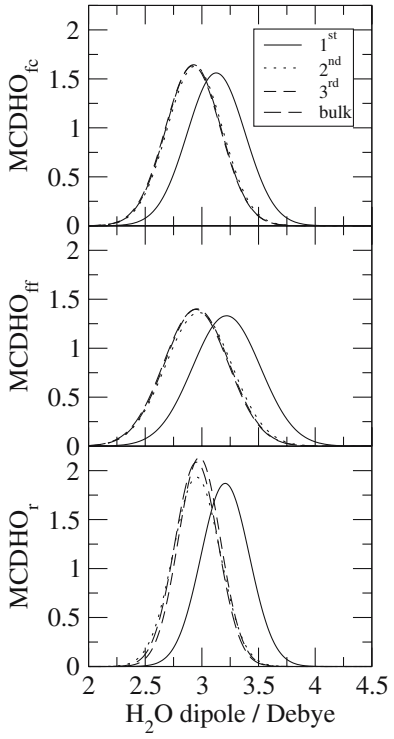

Fig. 10 Distributions of the dipole moment of each water molecule in the hydration shells and in the bulk as produced by the three polarizable models. The averages in the first shell are $\mu = 3.13$ D with MCDHO$_{fc}$, $\mu = 3.22$ D with MCDHO$_{ff}$, and $\mu = 3.21$ D with MCDHO$_r$. The bulk values of Ref. [75] are fully recovered at the second shell

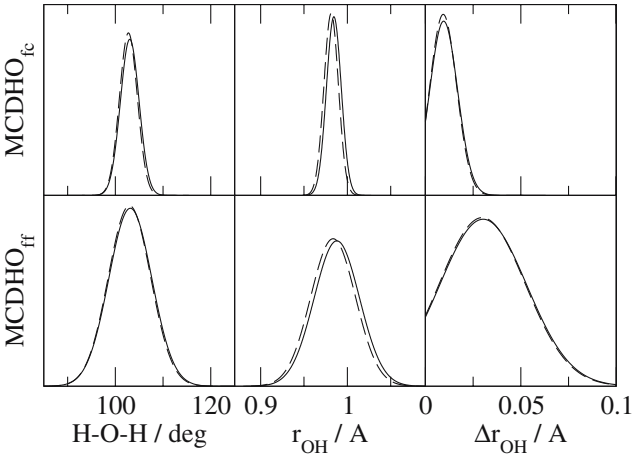

Fig. 11 Distributions of the $\widehat{\mathrm{HOH}}$ bond-angle (*left*) and r_{OH} bond-lengths (*middle*) of the water molecules in the first hydration shell (*continuous line*), compared to the bulk (*broken line*). The *right column* shows the distribution of the difference between the two r_{OH} bond-lengths of each molecule. The averages in the first hydration shell are slightly larger than in the bulk

4 Concluding remarks

For this study, a → c Li^+–H_2O analytical potential was fitted to ab initio calculations and to the experimentally determined

polarizability of the ion. This was employed with four versions of the MCDHO model for water [74,75] in numerical simulations of the diluted aqueous solution under ambient conditions. The good agreement with the experimental data validated the models, thus showing the reliability of their predictions. In particular, there is a clear convergence with other theoretical methods that predict a hydration number of four, even in much diluted solutions. Hence, the experimental determination of this value should be revised.

The interaction of Li^+ with its first hydration shell produces a very stable and rigid tetrahedral coordination. Though not to the same extent as Mg^{2+}, Li^+ behaves as a hydrated ion. It is likely to be modeled as a single entity using the hydrated ion model [67], which would prevent the appearance of five- and six-coordination that would arise from using effective pairwise potentials. The bulk water geometry should probably be used for the molecules in the hydrated ion model instead of the optimal geometries for the gas-phase cluster, as suggested by the results shown in Fig. 11.

The suite of models presented here performed well when reproducing experimental data and were in agreement with refined simulations. The good execution of the rigid polarizable $MCDHO_r$ model, which was also found in previous simulations [33], supports the view that bulk water geometry is quite stable. The nonpolarizable MCD model performs better than other simple pairwise potentials in regards to both energetic and structural predictions. In fact, its more than modest performance deserves some further comment, all the more so since the failure of effective pairwise potentials to describe aqueous solutions of ions has been well documented (see for instance [14]), especially on the subject of the hydration number. The results with the MCD model in this work also showed an overestimation that was, however, smaller than that of other models [81]. The other major discrepancies relative to the more complex models were the reduced stability of the tetrahedral arrangement of the first-shell water molecules and the enhanced alignment of their dipoles with the cation's electric field. The performance of the MCD model resembles that of the SPC/E [4] with the nonadditive ion-water potentials of Dang [15], which have been successfully applied to the study of aqueous solutions under different thermodynamic conditions [43,44,56,62]. Dang's potentials include explicit polarization and three-body terms to treat the nonadditive character of the water-ion-water interactions, and the SPC/E model takes into account the energetic cost of the polarization of the water molecules in the liquid phase. These features are intrinsically built in the MCDHO family of models [74], including MCD [75].

The failure of the nonpolarizable water models to correctly describe aqueous solutions of ions has been ascribed to their inability to respond to the ion's electric field, which should induce larger dipoles preferentially aligned to itself and thus produce repulsive dipole–dipole interactions [14]. This effect is usually minor for singly charged cations (see e.g. [9]). But in the case of Li^+ it is enhanced because of the short ion–water distance. The results of Fig. 10 in this work are consistent with this interpretation, since they show a significantly larger dipole moment of the first-shell water molecules in relation to those in the bulk.

Acknowledgements This work was supported by CONACyT (Grant No. G-33662-E) and DGAPA-UNAM (Grant No. IN118602).

References

1. Ayala R, Martínez JM, Pappalardo RR, Saint-Martin H, Ortega-Blake I, Sánchez-Marcos E (2002) Development of first-principles interaction model potentials. an application to the study of the bromide hydration. J Chem Phys 117(23):10512–10524
2. Ayala R, Martínez JM, Pappalardo RR, Sánchez-Marcos E (2003) On the halide hydration study: development of first-principles halide ion–water interaction potentials based on a polarizable model. J Chem Phys 119(18):9538–9548
3. Bader RFW (1995) Atoms in molecules. Oxford University Press, New York
4. Berendsen HJC, Grigera JR, Straatsma TP (1987) The missing term in effective pair potentials. J Phys Chem 91:6269–6271
5. Berendsen HJC, Postma JPM, van Gunsteren WF, Hermans J (1981) Interaction models for water in relation to protein hydration. In: Pullman B. (ed) Intermolecular forces. D. Reidel Publishing Company, Dordrecht, pp 331–342
6. Bernal-Uruchurtu MI, Ortega-Blake I (1995) Refined monte carlo study of Mg^{2+} and Ca^{2+} hydration. J Chem Phys 103:1588
7. Birch NJ (1999) Inorganic pharmacology of lithium. Chem Rev 99(9):2659–2682
8. Boys SF, Bernardi F (1970) The calculations of small molecular interactions by the differences of separate total energies. some procedures with reduced errors. Mol Phys 19(4):553–566
9. Carrillo-Tripp M, Saint-Martin H, Ortega-Blake I (2003) A comparative study of the hydration of Na^+ and K^+ with refined polarizable model potentials. J Chem Phys 118(15):7062–7073
10. Carrillo-Tripp M, Saint-Martin H, Ortega-Blake I (2004) Minimalist molecular model for nanopore selectivity. Phys Rev Lett 93(16):168104
11. Cartailler T, Kunz W, Turq P, Bellissent-Funel MC (1991) Lithium bromide in acetonitrile and water – a neutron-scattering study. J Phys Condens Matter 3(47)9511–9520
12. Chen B, Potoff JJ, Siepmann J.I (2000) Adiabatic nuclear and electronic sampling monte carlo simulations in the gibbs ensemble: application to polarizable force fields for water. J Phys Chem B 104:2378–2390
13. Coe JV (1994) Connecting cluster ions and bulk aqueous solvation, a new determination of bulk single ion solvation enthalpies. Chem Phys Lett 229:161–168
14. Curtiss LA, Woods-Halley J, Hautman J, Rahman A (1987) Nonadditivity of ab initio pair potentials for molecular dynamics of multivalent transition metal ions in water. J Chem Phys 86(4):2319–2327
15. Dang LX (1992) Development of nonadditive intermolecular potentials using molecular dynamics: solvation of Li^+ and F^- ions in polarizable water. J Chem Phys 96(9):6970–6977
16. Degrève L, de Pauli VM, Duarte MA (1997) Simulation study of the role and structure of monatomic ions multiple hydration shells. J Chem Phys 106(2):655–665
17. Duan Z, Zhang Z (2003) Solvation properties of Li^+ and Cl^- in water: molecular dynamics simulation with a non-rigid model. Mol Phys 101(10):1501–1510
18. Džidić I, Kebarle P (1970) Hydration of the alkali ions in the gas phase, enthalpies and entropies of reactions $M^+(H_2O)_{n-1} + H_sO \rightarrow M^+(H_2O)_n$. J Phys Chem 74(7):1466–1474
19. Evans R (1998) Mol Sim 4:409
20. Ewald PP (1921) Die berechnung optischer und elektrostatischer Gitterpotentiale. Ann Phys 64:253–287

21. Feller D, Glendening ED, Kendall RA, Peterson KA (1994) An extended basis set ab initio study of $Li^+(H_2O)_n$, $n = 1 - 6$. J Chem Phys 100(7):4981–4997
22. Feller D, Glendening ED, Woon DE, Feyereisen MW (1995) An extended basis set ab initio study of alkali metal cation-water clusters. J Chem Phys 103(9):3526–3642
23. Flyvbjerg H, Petersen HG (1989) Error-estimates on averages of correlated data. J Chem Phys 91(1):461–466
24. Frisch MJ, Trucks GW, Schlegel HB, Scuseria GE, Robb MA, Cheeseman JR, Zakrzewski VG, J. A. Montgomery J, Stratmann R.E, Burant JC, Dapprich S, Millam JM, Daniels AD, Kudin KN, Strain MC, Farkas O, Tomasi J, Barone V, Cossi M, Cammi R, Mennucci B, Pomelli C, Adamo C, Clifford S, Ochterski, J, Petersson GA, Ayala PY, Cui Q, Morokuma K, Malick DK, Rabuck AD, Raghavachari K, Foresman JB, Cioslowski J, Ortiz JV, Baboul AG, Stefanov BB, Liu G, Liashenko A, Piskorz P, Komaromi I, Gomperts R, Martin RL, Fox DJ, Keith T, Al-Laham MA, Peng CY, Nanayakkara A, Gonzalez C, Challacombe M, Gill PMW, Johnson B, Chen W, Wong MW, Andres JL, Gonzalez C, Head-Gordon M, Replogle ES, Pople JA (1998) Gaussian 98, Revision A.7. Gaussian, Inc, Pittsburgh PA
25. Glendening ED, Feller D (1995) Cation-water interactions: The $M^+(H_2O)_n$ clusters for alkali metals, M = Li, Na, K, Rb and Cs. J Phys Chem 99:3060–3067
26. Grossfield A (2005) Dependence of ion hydration on the sign of the ion's charge. J Chem Phys 122:024 506
27. Hannongbua S (1997) The role of nonadditive effects in the first solvation shell of Na^+ and Mg^{2+} in liquid ammonia: Monte carlo studies including three-body corrections. J Chem Phys 106(14):6076–6081
28. Hannongbua S (1998) On the solvation of lithium ions in liquid ammonia: Monte carlo simulations with a three-body potential. Chem Phys Lett 288(5–6):663–668
29. Hastings WK (1970) Monte carlo sampling methods using markov chains and their applications. Biometrika 57:92–109
30. Helm L, Merbach AE (1999) Water exchange on metal ions: experiments and simulations. Coord Chem Rev 187:151–181
31. Hernández-Cobos J, Ortega-Blake I (1995) Hydrophobic hydration in methanol aqueous-solutions. J Chem Phys 103(21):9261–9273
32. Hernández-Cobos J, Ortega-Blake I, Bonilla-Marín M, Moren o-Bello M (1993) A refined monte-carlo study of aqueous urea solutions. J Chem Phys 99(11):9122–9134
33. Hernández-Cobos J, Saint-Martin H, Mackie AD, Vega LF, Ortega-Blake I (2005) Water-liquid vapor equilibria predicted by refined ab initio derived potentials. J Chem Phys 123(4):044 506
34. Hess B, Saint-Martin H, Berendsen HJC (2002) Flexible constraints: an adiabatic treatment of quantum degrees of freedom, with application to the flexible and polarizable mobile charge densities in harmonic oscillators model for water. J Chem Phys 116(22):9602–9610
35. Howell I, Nielson GW (1996) Li^+ hydration in concentrated aqueous solution. J Phys Condens Matter 8:4455–4463
36. Imberti S, Botti A, Bruni F, Cappa G, Ricci MA, Soper AK (2005) Ions in water: the microscopic structure of concentrated hydroxide solutions. J Chem Phys 122:194 509
37. Jorgensen WL, Chandrasekhar J, Madura JD, Impey RW, Klein ML (1983) Comparison of simple potential functions for simulating liquid water. J Chem Phys 79:926–935
38. Kameda Y, Usuki T, Uemura O (1999) The structure analysis of highly concentrated Li-salt solutions. High Temperature Materials and Processes 18(1–2):27–40
39. Karpov GV (2005) On the structure of hydration shells of alkali metal ions in aqueous solution. Chem Phys Lett 402(4–6):300–305
40. Klots CE (1981) Solubility of protons in water. J Chem Phys 85:3585–3588
41. Kochanski E (1987) Nonadditivity of SCF interaction energies in $H_3O^+(H_2O)_2$. Chem Phys Lett 133(2):143–149
42. Kowall T, Foglia F, Helm L, Merbach AE (1995) Molecular-dynamics simulation study of lanthanide ions Ln^{3+} in aqueous–solution including water polarization – change in coordination-number from 9 to 8 along the series. J Am Chem Soc 117(13): 3790–3799
43. Lee SH (2003) Molecular dynamics simulation of limiting conductance for Li^+ ion in supercritical water using polarizable models. Mol Sim 29(3):211 –221
44. Lee SH, Rasaiah JC (1996) Molecular dynamics simulation of ion mobility. 2. Alkali metal and halide ions using the SPC/E model for water at 25°C. J Phys Chem 100:1420–1425
45. Loeffler HH, Rode BM (2002) The hydration structure of the lithium ion. J Chem Phys 117(1):110–117
46. Lotrich VF, Salewicz K (1997) Symmetry-adapted perturbation theory of three-body nonadditivity of intermolecular interaction energy. J Chem Phys 106(23):9668–9687
47. Lyubartsev AP, Laaksonen A (2000) Determination of effective pair potentials from ab initio simulations: application to liquid water. Chem Phys Lett 325(1–3):15–21
48. Lyubartsev AP, Laasonen K, Laaksonen A (2001) Hydration of Li^+ ion, an ab initio molecular dynamics simulation. J Chem Phys 114(7):3120–3126
49. van-der Maarel JRC, Powell DH, Jawahier AK, Leyte-Zuiderweg LH, Nielson GW, Bellissent-Funel MC (1989) On the structure and dynamics of lithium counterions in poly-electrolyte solutions – a nuclear magnetic-resonance and neutron-scattering study. J Chem Phys 90(11):6709–6715
50. Marcus Y (1994) A simple empirical model describing the thermodynamics of hydration of ions of widely varying charges, sizes and shapes. Biophys Chem 51:111–127
51. Marcus Y (1997) Ion properties. Marcel Dekker, Inc, New York
52. Martin MG, Chen B, Siepmann JI (1998) A novel Monte Carlo algorithm for polarizable force fields: application to a fluctuating charge model for water. J Chem Phys 108(9):3383–3385
53. Martínez JM, Hernández-Cobos J, Saint-Martin H, Pappalardo RR, Ortega-Blake I, Sánchez-Marcos E (2000) Coupling a polarizable model to the hydrated ion – water interaction potential: a test on the Cr^{3+} hydration. J Chem Phys 112(5):2339–2347
54. Martínez JM, Pappalardo RR, Sánchez-Marcos E (1998) A molecular dynamics study of the Cr^{3+} hydration based on a fully flexible hydrated ion model. J Chem Phys 109(4):1445–1455
55. Martínez JM, Pappalardo RR, Sánchez-Marcos E (1999) Shape and size of simple cations in aqueous solutions: a theoretical reexamination of the hydrated ion via computer simulations. J Am Chem Soc 121(3):1669–1676
56. Masia M, Rey R (2003) Reaction rate theory approach to thermodynamic state dependence of hydration shell exchange for $Li^+(aq)$. J Phys Chem B 107:2651–2659
57. Metropolis N, Rosenbluth AW, Rosenbluth MN, Teller AH, Teller E (1953) Equations of state calculations by fast computing machines. J Chem Phys 21:1087–1089
58. Michaellian KH, Moskovits M (1978) Tetrahedral hydration of ions in solution. Nature 273:135–136
59. Narten AH, Vaslow F, Levy HA (1973) Diffraction pattern and structure of aqueous lithium-chloride solutions. J Chem Phys 58(11):5017–5023
60. Natália M, Cordeiro DS, Ignaczak A, Gomes JANF (1993) Simulation of water solutions of Ni^{2+} at infinite dilution. Chem Phys 176(1):97–108
61. Newsome JR, Nielson GW, Enderby JE (1980) Lithium ions in aqueous solution. J Phys C: Solid St Phys 13:L923–L926
62. Noworyta JP, Koneshan S, Rasaiah JC (2000) Dynamics of aqueous solutions of ions and neutral solutes at infinite dilution at a supercritical temperature of 683 K. J Am Chem Soc 122:11194–11 202
63. Öhrn A, Karlström G (2004) A combined quantum chemical statistical mechanical simulation of the hydration of Li^+, Na^+, F^- and Cl^-. J Phys Chem B 108:8452–8459
64. Ohtaki H, Radnai T (1993) Structure and dynamics of hydrated ions. Chem Rev 93(3):1157–1204
65. Ortega-Blake I, Hernández-Cobos J, Novaro O (1984) The role of nonadditive effects in the second hydration shell of Mg^{2+} and Ca^{2+} – a molecular-orbital study of the three-body potential-energy surface. J Chem Phys 81(4):1894–1900

66. Ortega-Blake I, Novaro O, Leś A, Rybak S (1982) A molecular-orbital study of the hydration of ions – the role of non-additive effects in the hydration shells around Mg^{2+} and Ca^{2+}. J Chem Phys 76(11):5405–5413
67. Pappalardo RR, Martínez JM, Sánchez-Marcos E (1996) Application of the hydrated ion concept for modeling aqueous solutions containing highly charged ions: a Monte Carlo simulation of Cr^{3+} in water using an ab initio intermolecular potential. J Phys Chem 100(28):11748–11 754
68. Pastor N, Ortega-Blake I (1993) On the existence of very large nonadditivities for clusters of distorted water molecules. J Chem Phys 99(10):7899–7906
69. Pettitt BM, Rossky PJ (1986) Alkali-halides in water – ion solvent correlations and ion-ion potentials of mean force at infinite dilution. J Chem Phys 84(10):5836–5844
70. Reimers JR, Watts RO, Klein ML (1982) Intermolecular potential functions and the properties of water. Chem Phys 64(1):95–114
71. Rempe SB, Pratt LR, Hummer G, Kress JD, Martin RL, Redondo A (2000) The hydration number of Li^+ in liquid water. J Am Chem Soc 122:966–967
72. Rodgers MT, Armentrout PB (1997) Collision-induced dissociation measurements on $Li^+(H_2O)_n, n = 1–6$: the first direct measurement of the $Li^+–OH_2$ bond energy. J Phys Chem A 101:1238–1249
73. Rudolph W, Brooker MH, Pye CC (1995) Hydration of lithium ion in aqueous-solution. J Phys Chem 99(11):3793–3797
74. Saint-Martin H, Hernández-Cobos J, Bernal-Uruchurtu MI, Ortega-Blake I, Berendsen HJC (2000) A mobile charge densities in harmonic oscillators (MCDHO) molecular model for numerical simulations: the water-water interaction. J Chem Phys 113(24):10899–10912
75. Saint-Martin H, Hernández-Cobos J, Ortega-Blake I (2005) Water potentials based on a single potential energy surface and different molecular degrees of freedom. J Chem Phys 122(22):224–509
76. Saint-Martin H, Hess B, Berendsen HJC (2004) An application of flexible constraints in monte carlo simulations of the isobaric-isothermal ensemble of liquid water and ice Ih with the polarizable and flexible MCDHO model. J Chem Phys 120(23):11133–11143
77. SanRomán-Zimbrón ML, Ortega-Blake I (1997) On the molecular basis of hydrophobicity: A Monte Carlo study of propionic acid hydration. J Chem Phys 107(8):3253–3261
78. Schmid R, Miah AM, Sapunov VN (2000) A new table of the thermodynamic quantities of ionic hydration: values and some applications (enthalpy–entropy compensation and born radii). Phys Chem Chem Phys 2:97–102
79. Soper AK (1996) Empirical potential monte carlo simulation of fluid structure. Chem Phys 202:295–306
80. Soper AK (2001) Tests of the empirical potential structure refinement method and a new method of application to neutron diffraction data on water. Mol Phys 99(17):1503–1516
81. Spångberg D, Hermansson K (2003) Effective three-body potentials for Li^+(aq) and Mg^{2+}(aq). J Chem Phys 119(14):7263–7281
82. Spångberg D, Hermansson K (2004) Many-body potentials for aqueous Li^+, Na^+, Mg^{2+}, and Al^{3+}: comparison of effective three-body potentials and polarizable models. J Chem Phys 120(10):4829–4843
83. Tissandier MD, Cowen KA, Feng WY, Gundlach E, Cohen MH, Earhart AD, Coe JV, Jr TRT (1998) The proton's absolute aqueous enthalpy and gibbs free energy of solvation from cluster-ion solvation data. J Phys Chem A 102:7787–7794
84. Tóth G (1996) Ab initio pair potential parameter set for the interaction of a rigid and a flexible water model and the complete series of the halides and alkali cations. J Chem Phys 105(13):5518–5524
85. Yamagami M, Yamaguchi T, Wakita H, Misawa M (1994) Pulsed-neutron diffraction study on lithium-(i) hydration in supercooled aqueous chloride solutions. J Chem Phys 100(4):3122–3126
86. Zhou J, Lu X, Wang Y, Shi J (2002) Molecular dynamics study on ionic hydration. Fluid Phase Equil 194–197:257–270